Inorg. Chem. **2003**, *42*, 4817−4827

Binuclear Manganese Compounds of Potential Biological Significance. Part 2. Mechanistic Study of Hydrogen Peroxide Disproportionation by Dimanganese Complexes: The Two Oxygen Atoms of the Peroxide End up in a Dioxo Intermediate

Lionel Dubois,[†] Régis Caspar,[†] Lilian Jacquamet,[‡] Pierre-Emmanuel Petit,[‡] Marie-France Charlot,[§] Carole Baffert,[||] Marie-Noëlle Collomb,[||] Alain Deronzier,[||] and Jean-Marc Latour*,[†]

Laboratoire de Physicochimie des Métaux en Biologie, FRE 2427 CEA-CNRS-UJF, CEA-Grenoble, 38054 Grenoble Cedex 9, France, European Synchrotron Radiation Facility, Grenoble, France, Laboratoire d'Electrochimie Organique et de Photochimie Rédox, UMR CNRS 5630, Université Joseph Fourier Grenoble 1, B.P. 53 38041 Grenoble Cedex 9, France, and Laboratoire de Chimie Inorganique, UMR 8613, Université de Paris Sud-Orsay, 91405 Orsay Cedex, France

Received October 30, 2002

The dimanganese(II,II) complexes **1a** $[Mn_2(L)(OAc)_2(CH_3OH)](ClO_4)$ and **1b** $[Mn_2(L)(OBz)_2(H_2O)](ClO_4)$, where HL is the unsymmetrical phenol ligand 2-(bis-(2-pyridylmethyl)aminomethyl)-6-((2-pyridylmethyl)(benzyl)aminomethyl)-4-methylphenol, react with hydrogen peroxide in acetonitrile solution. The disproportionation reaction was monitored by electrospray ionization mass spectrometry (ESI-MS) and EPR and UV–visible spectroscopies. Extensive EPR studies have shown that a species (**2**) exhibiting a 16-line spectrum at $g \sim 2$ persists during catalysis. ESI-MS experiments conducted similarly during catalysis associate **2a** with a peak at 729 (791 for **2b**) corresponding to the formula $[Mn^{III}Mn^{IV}(L)(O)_2(OAc)]^+$ ($[Mn^{III}Mn^{IV}(L)(O)_2(OBz)]^+$ for **2b**). At the end of the reaction, it is partly replaced by a species (**3**) possessing a broad unfeatured signal at $g \sim 2$. ESI-MS associates **3a** with a peak at 713 (775 for **3b**) corresponding to the formula $[Mn^{II}Mn^{III}(L)(O)(OAc)]^+$ ($[Mn^{II}Mn^{III}(L)(O)(OBz)]^+$ for **3b**). In the presence of $H_2{}^{18}O$, these two peaks move to 733 and to 715 indicating the presence of two and one oxo ligands, respectively. When $H_2{}^{18}O_2$ is used, **2a** and **3a** are labeled showing that the oxo ligands come from H_2O_2. Interestingly, when an equimolar mixture of H_2O_2 and $H_2{}^{18}O_2$ is used, only unlabeled and doubly labeled **2a**/**b** are formed, showing that its two oxo ligands come from the same H_2O_2 molecule. All these experiments lead to attribute the formula $[Mn^{III}Mn^{IV}(L)(O)_2(OAc)]^+$ to **2a** and to **3a** the formula $[Mn^{II}Mn^{III}(L)(O)(OAc)]^+$. Freeze–quench/EPR experiments revealed that **2a** appears at 500 ms and that another species with a 6-line spectrum is formed transiently at ca. 100 ms. **2a** was prepared by reaction of **1a** with *tert*-butyl hydroperoxide as shown by EPR and UV–visible spectroscopies and ESI-MS experiments. Its structure was studied by X-ray absorption experiments which revealed the presence of two or three O atoms at 1.87 Å and three or two N/O atoms at 2.14 Å. In addition one N atom was found at a longer distance (2.3 Å) and one Mn at 2.63 Å. **2a** can be one-electron oxidized at $E_{1/2} = 0.91$ V_{NHE} ($\Delta E_{1/2} = 0.08$ V) leading to its $Mn^{IV}Mn^{IV}$ analogue. The formation of **2a** from **1a** was monitored by UV–visible and X-ray absorption spectroscopies. Both concur to show that an intermediate $Mn^{II}Mn^{III}$ species, resembling **4a** $[Mn_2(L)(OAc)_2(H_2O)](ClO_4)_2$, the one-electron-oxidized form of **1a**, is formed initially and transforms into **2a**. The structures of the active intermediates **2** and **3** are discussed in light of their spectroscopic properties, and potential mechanisms are considered and discussed in the context of the biological reaction.

The catalase enzymes play a pivotal role in the protection of living cells against oxidative stress by eliminating hydrogen peroxide before its reduction gives rise to the deleterious hydroxyl radical.[1,2] While most of these enzymes are hemoproteins, a few of them of bacterial origin involve

* To whom correspondence should be addressed. Tel: (33) 4 38 78 44 07. Fax: (33) 4 38 78 34 62. E-mail: jlatour@cea.fr.
[†] CEA-Grenoble.
[‡] European Synchrotron Radiation Facility.
[§] Université de Paris Sud-Orsay.
[||] Université Joseph Fourier Grenoble 1.

(1) Halliwell, B.; Gutteridge, J. M. C. *Methods in Enzymology*; Academic Press: San Diego, 1990, pp 1−85.
(2) Stadtman, E. R.; Berlett, P. B.; Chock, P. B. *Proc. Natl. Acad. Sci. U.S.A.* **1990**, *87*, 384−388.

10.1021/ic020646n CCC: $25.00
Published on Web 07/04/2003

manganese as a cofactor.[3] Recent crystallographic studies have revealed that the active sites of the Mn enzymes found in the bacteria *Thermus thermophilus*[4] and *Lactobacillus plantarum*[5] comprise two manganese atoms triply bridged by the carboxylate group of a glutamate and two water-derived ligands. Biochemical[6] and spectroscopic studies[7] have shown that during catalysis this capped diamond core shuttles between the oxidation states $Mn^{II}Mn^{II}$ and $Mn^{III}Mn^{III}$. Nevertheless, owing to the fast kinetics of the enzymatic reaction ($k_{cat} \sim 10^5\ s^{-1}$)[8] and the fact that the oxidized and the reduced forms both react with the same substrate (H_2O_2), mechanistic studies have been very limited. Therefore most of the mechanistic hypotheses have been based on studies of biomimetic compounds.[9−11] In this respect, it is worth noting that two recent hypotheses involve a $\mu_{1,1}$-hydroperoxide as a key intermediate.[9,12] The most detailed mechanistic studies were performed on complexes of ligands involving either alcoholates[9,13] or phenolates[11,14] which stabilize the dimanganese unit by providing it with an internal bridge. Depending upon the Mn ligands, all oxidation states of the pair from $Mn^{II}Mn^{II}$ to $Mn^{IV}Mn^{IV}$ have been implicated in the catalysis.

In the case of dimanganese complexes of pentadentate bisaminoalkyliminophenol ligands, the involvement of oxomanganese(IV) species has been demonstrated by Okawa et al.[14] through the observation in DMF of a characteristic vibronically split electronic absorption of the $Mn^{IV}(O)$ unit. $Mn^{II}Mn^{IV}(O)$ and $Mn^{IV}(O)Mn^{IV}(O)$ species were proposed to be the active species in the catalase-like reaction. On the other hand, Nishida et al. failed to detect the characteristic absorption of the oxomanganese(IV) unit and cast doubt on its occurrence.[15] Instead, they provided EPR evidence of the formation of a di(μ-oxo)dimanganese(III,IV) species in the reaction of hydrogen peroxide with dimanganese complexes of heptadentate hexaaminophenols but did not establish definitely whether this species is a catalytic intermediate or a mere byproduct.

In this article, we show that the hydrogen peroxide disproportionation induced by dimanganese(II,II) com-

Scheme 1

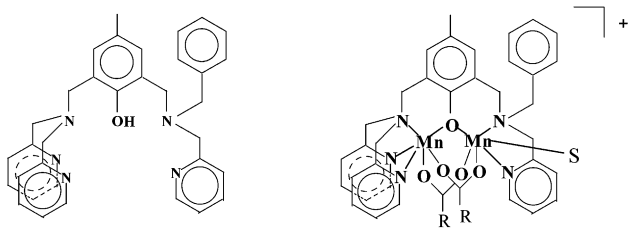

HL

1a: R = Me, S = CH_3OH
1b: R = Ph, S = H_2O

Scheme 2

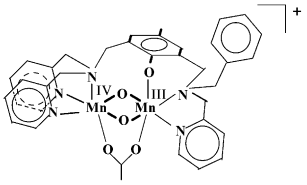

plexes[16] of the unsymmetrical phenolate ligand 2-[(bis(2-pyridylmethyl)amino)methyl]-6-[((2-pyridylmethyl) (benzyl)-amino)methyl]-4-methylphenol (HL, Scheme 1) involves a di(μ-oxo)dimanganese(III,IV) intermediate. Indeed, when the dimanganese(II,II) complexes **1a** $[Mn_2(L)(OAc)_2(CH_3OH)](ClO_4)$ and **1b** $[Mn_2(L)(OBz)_2(H_2O)](ClO_4)$ (Scheme 1) are reacted with H_2O_2, monitoring the reaction using a combination of electrospray ionization mass spectrometry (ESI-MS) and EPR spectroscopy reveals that the system involves two active species: a dioxodimanganese(III,IV) species **2** and an oxodimanganese(II,III) **3** one. In this article, we report also the independent synthesis of the active dioxodimanganese(III,IV) complex **2a** derived from **1a** and its structural and spectroscopic characterization which shows that to accommodate the Mn_2O_2 core the phenolic ligand changes its usual bridging coordination mode (Scheme 2). Moreover, labeling experiments coupled to ESI-MS revealed that the two oxo ligands in **2a** come from the same peroxide molecule, a feature inconsistent with the occurrence of a $\mu_{1,1}$-hydroperoxide intermediate.

Experimental Section

Materials. $H_2{}^{18}O$ (95% ^{18}O) and $H_2{}^{18}O_2$ (90% ^{18}O, 2.2% in H_2O) were obtained from Eurisotope and Leman, respectively. All reagents were used as received. The compounds **5** $[Mn_2(O)_2(OAc)(bpea)_2](PF_6)_2$[17] (bpea = bis-2-picolylethylamine) and **6** $[Mn_2(O)_2(tpa)_2](ClO_4)_3$[18] (tpa = tris-2-picolylamine) were prepared according to literature procedures.

Synthesis. The ligand HL,[19] the dimanganese(II,II) complexes $[Mn_2(L)(OAc)_2(CH_3OH)](ClO_4)$ **1a** and $[Mn_2(L)(OBz)_2(H_2O)](ClO_4)$ **1b**, and the dimanganese(II,III) complex $[Mn_2(L)(OAc)_2(H_2O)](ClO_4)_2$ **4a**[16] were synthesized as described earlier.

(3) Dismukes, G. C. *Chem. Rev.* **1996**, *96*, 2909−2926.
(4) Antonyuk, S. V.; Melik-Adamyan, V. R.; Popov, A. N.; Lamzin, V. S.; Hempstead, P. D.; Harrison, P. M.; Artymyuk, P. J.; Barynin, V. V. *Crystallogr. Rep. (Transl. Kristallografiya)* **2000**, *45*, 105−116.
(5) Barynin, V. V.; Whittaker, M. M.; Antonyuk, S. V.; Lamzin, V. S.; Harrison, P. M.; Artymiuk, P. J.; Whittaker, J. *Structure* **2001**, *9*, 725−738.
(6) Khangulov, S. V.; Barynin, V. V.; Antonyuk-Barynina, S. V. *Biochim. Biophys. Acta* **1990**, *1020*, 25−33.
(7) Waldo, G. S.; Penner-Hahn, J. E. *Biochemistry* **1995**, *34*, 1507−1512.
(8) Shank, M.; Barynin, V.; Dismukes, G. *Biochemistry* **1994**, *33*, 15433−15436.
(9) Boelrijk, A. E. M.; Dismukes, G. C. *Inorg. Chem.* **2000**, *39*, 3020−3028.
(10) Pecoraro, V. L.; Baldwin, M. J.; Gelasco, A. *Chem. Rev.* **1994**, *94*, 807−826.
(11) Okawa, H.; Sakiyama, H. *Pure Appl. Chem.* **1995**, *67*, 273−280.
(12) Whittaker, M.; Barynin, V. V.; Antonyuk, S. V.; Whittaker, J. W. *Biochemistry* **1999**, *38*, 9126−9136.
(13) Gelasco, A.; Bensiek, S.; Pecoraro, V. L. *Inorg. Chem.* **1998**, *37*, 3301−3309.
(14) Wada, H.; Motoda, K. I.; Ohba, M.; Sakiyama, H.; Matsumoto, N.; Okawa, H. *Bull. Chem. Soc. Jpn.* **1995**, *68*, 1105−1114.
(15) Sasaki, Y.; Akamatsu, T.; Tsuchiya, K.; Ohba, S.; Sakamoto, M.; Nishida, Y. *Polyhedron* **1998**, *17*, 235−242.
(16) Dubois, L.; Xiang, D. F.; Tan, X. S.; Pécaut, J.; Jones, P.; Baudron, S.; Le Pape, L.; Baffert, C.; Chardon-Noblat, S.; Collomb, M. N.; Deronzier, A.; Latour, J. M. *Inorg. Chem.* **2003**, *42*, 750−760.
(17) Pal, S.; Olmstead, M. M.; Armstrong, W. H. *Inorg. Chem.* **1995**, *34*, 4708−4715.
(18) Towle, D. K.; Botsford, C. A.; Hodgson, D. J. *Inorg. Chim. Acta* **1988**, *141*, 167−168.
(19) Lambert, E.; Chabut, B.; Chardon-Noblat, S.; Deronzier, A.; Chottard, G.; Bousseksou, A.; Tuchagues, J. P.; Bardet, M.; Laugier, J.; Latour, J. M. *J. Am. Chem. Soc.* **1997**, *119*, 9424−9437.

Synthesis of 2a. Complex **1a** (10 mg) was dissolved in 10 mL of acetonitrile and the mixture cooled to −20 °C. To this solution was added 10 μL of a 70% (7.2 M) aqueous solution of *tert*-butyl hydroperoxide. After 10−15 min, the solution turned dark brown. The reaction mixture was filtered and then evaporated to dryness at ca. −5 °C with a vacuum pump to furnish a brown solid (7 mg).

CAUTION! Perchlorate salts of metal complexes with organic ligands are potentially explosive.

Spectroscopic Measurements. Electronic absorption spectra were recorded on a Hewlett-Packard HP 89090A diode array spectrophotometer. Electrospray ionization mass spectra were obtained with a LCQ Finnigan Thermoquest ESI source spectrometer with an ion trap and an octupolar analyzer. EPR spectra at X band were recorded with an EMX Bruker spectrometer equipped with an Oxford Instrument cryostat ESR900. All spectra presented have been recorded with the following set of conditions: $T = 10$ K, $P = 0.2$ mW, modulation $F = 100$ kHz, $I = 9$ G. Freeze−quench experiments were performed with a model 715 apparatus from Update Instrument, Inc. The freezing solvent was isopentane maintained at −150 °C by circulating liquid nitrogen. Electrochemical measurements were performed as already described.[20]

X-ray Absorption Spectroscopy Measurements. XAS spectra at the Mn K-edge were collected at the European Synchrotron Radiation Facility (ESRF, Grenoble, France), on the undulator beamline ID26.[21] The storage ring operating conditions were 6 GeV electron energy and 150−185 mA electron current. A Si(220) double-crystal monochromator was used for these experiments. The beamline was first calibrated at the Cu K-edge based on an absolute calibration of the first inflection point of the Cu foil K-edge at 8983.32 eV.[22] Then, for all experiments, a reference foil of metallic Mn was used to provide an internal and accurate energy calibration of the monochromator for all spectra. The first inflection point of the Mn K-edge was set at 6539 eV. The energy reproducibility for these experiments was ±0.05 eV. Two mirrors (amorphous silicon before, and SiO_2 after the monochromator) were used to remove the high-energy harmonics from the incident X-ray beam (cutting energy at 8 keV). XAS data for model compounds were collected in the transmission mode. For solution samples with low Mn concentrations, XAS spectra were collected in the fluorescence mode with the sample positioned 45° with respect to the beam to minimize elastic scattering. The fluorescence yield was measured as a function of X-ray energy using a pin-diode detector. A Cr_2O_3 filter (6 μ absorbance) was used to further minimize unwanted elastic scattering. XAS spectra were collected from 6440 to 7440 eV at 20 K.

The appropriate amounts of powdered model compounds (size fraction below 50 μm) were mixed with boron nitride to reach an edge jump ($\Delta\mu/\mu$) close to 1. After mixing during 12 h to homogenize the sample, it was pelletized and loaded into a Teflon sample holder. The samples used to study the formation of **2a** were prepared in a 1/1 mixture of toluene and acetonitrile. The reaction of **1a** (1 mM) with 7 equiv of TBHP was done at −10 °C, and aliquots were taken at chosen time intervals, syringed into the sample holder, and frozen in liquid nitrogen.

Data analysis was made as previously described[23,24] with the SEDEM software package.[25] As a measure of the sample integrity, we compared the absorption spectra measured for the first and the last scan of each sample. No spectral changes were observed over the course of the data collection, indicating that no change is occurring around the metal center.

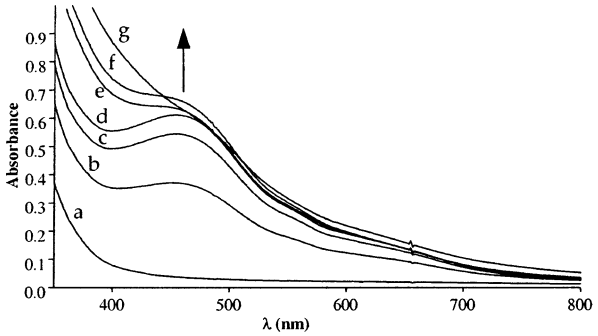

Figure 1. UV−visible monitoring of H_2O_2 disproportionation by **1a**. The different curves (spectra a−g) are recorded after $t = 0$, 10 s, 30 s, 70 s, 20 min, 30 min, and 50 min. ([**1a**] = 0.6 mM, [H_2O_2] = 230 mM, $T = 0$ °C.)

The structural parameters were obtained as described earlier.[23,24] Ab initio calculations were performed with the FEFF 7.02 code[26] for a single absorber−scatterer pair Mn−O at 1.80 Å distance, a single Mn−N interaction at 2.10 Å, and a single Mn−Mn interaction at 2.65 Å. Since N_i and σ_i^2 are strongly correlated, N_i was held fixed to chemically reasonable integer values and only R_i and σ_i^2 were optimized.

Results

Synthesis. When the ligand H(L)[19] is reacted with $Mn(H_2O)_4(OAc)_2$ or with $Mn(H_2O)_6(ClO_4)_2$ in the presence of NaOBz, the dimanganese(II,II) compounds $[Mn_2(L)(OAc)_2(CH_3OH)](ClO_4)$ **1a** and $[Mn_2(L)(OBz)_2(H_2O)](ClO_4)$ **1b** are obtained. The two compounds have been characterized by crystallography and spectroscopic and electrochemical techniques.[16] They are illustrated in Scheme 1.

Spectroscopic Monitoring of the Catalase-like Reaction. When either of the two complexes **1a**,**b** is reacted with H_2O_2 in acetonitrile at room temperature, the colorless solution becomes dark brown while a vigorous evolution of dioxygen is observed instantaneously. In order to get an insight into the mechanism of this reaction, it was monitored by using a combination of electronic absorption and EPR spectroscopies and electrospray ionization mass spectrometry.

UV−Visible Spectroscopy. Addition of H_2O_2 (380 equiv) to a 0.6 mM solution of **1a** causes the immediate appearance of a strong visible absorption near 450 nm flanked by two low-energy shoulders at ca. 550 and 650 nm (Figure 1). At 20 °C, the absorption is stable after ca. 1 min. Similar observations are made for **1b**, but the corresponding bands are about 3 times less intense and their rate of formation is slower since the absorption plateau is reached only after ca. 3 min. Two types of binuclear manganese complexes are known to possess such a set of three absorptions: these are

(20) Romero, I.; Dubois, L.; Collomb, M. N.; Deronzier, A.; Latour, J. M.; Pecaut, J. *Inorg. Chem.* **2002**, *41*, 1795−1806.
(21) Gauthier, C.; Solé, V.; Signorato, R.; Goulon, J.; Moguiline, E. *J. Synchrotron Radiat.* **1999**, *6*, 164−166.
(22) Pettitfer, R.; Hermes, C. *J. Appl. Crystallogr.* **1985**, *18*, 404−412.
(23) Adrait, A.; Le Pape, L.; Gonzalès de Peredo, A.; Aberdam, D.; Hazemann, J. L.; Latour, J. M.; Michaud-Soret, I. *Biochemistry* **1999**, *38*, 6248−6260.
(24) Jacquamet, L.; Dole, F.; Jeandey, C.; Oddou, J. L.; Perret, E.; Le Pape, L.; Aberdam, D.; Hazemann, J. L.; Michaud-Soret, I.; Latour, J. M. *J. Am. Chem. Soc.* **2000**, *122*, 394−395.
(25) Aberdam, A. *J. Synchrotron Radiat.* **1998**, *5*, 1287−1297.
(26) Zabinsky, S.; Rehr, J.; Ankudinov, A.; Albers, R.; Eller, M. J. *Phys. Rev. B* **1995**, *52*, 2995−3009.

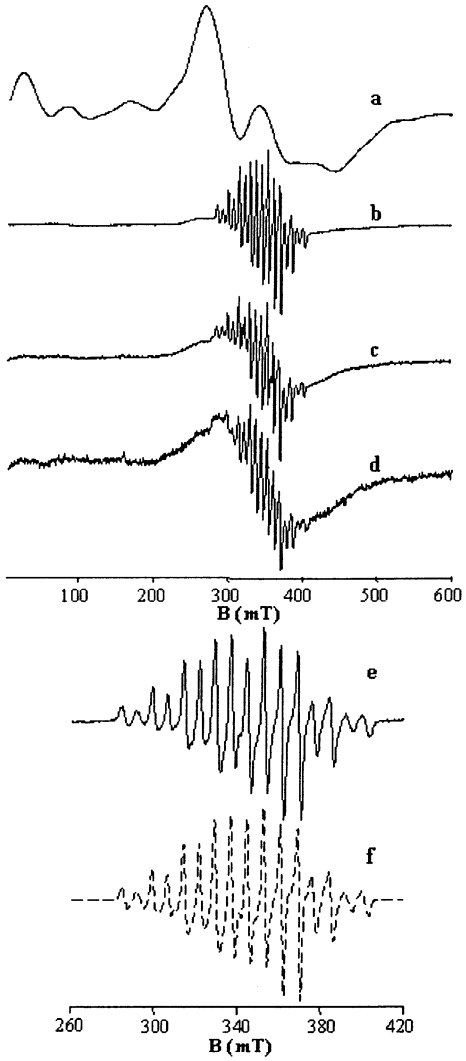

Figure 2. EPR spectra of the reaction of **1a** in acetonitrile with H_2O_2 and EPR spectrum of **2a** in acetonitrile. Spectra a−d: reaction times 0, 5, 10 and 50 min; reaction conditions, [**1a**] = 0.6 mM, [H_2O_2] = 460 mM, T = − 10 °C. Spectra e and f: experimental and simulated spectra of **2a** (see Table 1 for simulation parameters, frequency 9.656 GHz).

phenoxo bridged $Mn^{II}Mn^{III}$ complexes and the bis(μ-oxo)-$Mn^{III}Mn^{IV}$ complexes.[27]

EPR Spectroscopy. We made an extensive use of EPR spectroscopy to investigate the reaction at various time scales and under various conditions differing by the H_2O_2/complex ratio and the presence of acid or base. Figure 2 illustrates the EPR spectra recorded before and between 5 and 50 min after addition of H_2O_2 to an acetonitrile solution of **1a** at −10 °C. The characteristic very broad spectrum of **1a** (Figure 2a) disappears and is rapidly replaced by a 16-line spectrum centered near $g = 2$. After 5 min the spectrum of **1a** has almost completely disappeared (Figure 2b) and the new spectrum is fully developed. At longer times this spectrum persists, but after 10 min a new spectrum centered near $g =$ 2 starts growing (Figure 2c,d). This spectrum extends from 2200 to 4600 G and lacks hyperfine features. Identical observations are made for the reaction of H_2O_2 with **1b**

(27) Gamelin, D. R.; Kirk, M. L.; Stemmler, T. L.; Pal, S.; Armstrong, W. H.; Penner-Hahn, J. E.; Solomon, E. I. *J. Am. Chem. Soc.* **1994**, *116*, 2392−2399.

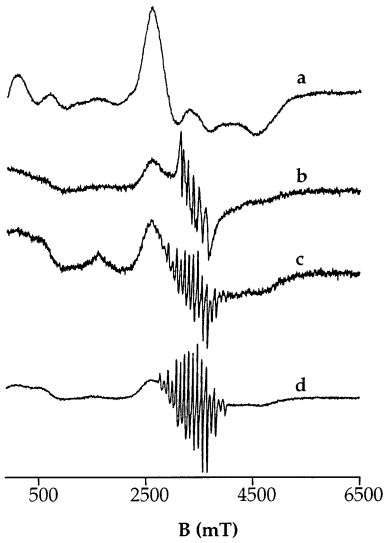

Figure 3. EPR spectra of the reaction of **1a** in acetonitrile with H_2O_2. Spectra a−d: reaction times 0, 100 ms, 750 ms and 1.5 s; reaction conditions, [**1a**] = 1.0 mM, [H_2O_2] = 460 mM, T = 20 °C.

except for a slower development of the two new spectra and the longer persistence of that of **1b**. When **1a** is reacted with only 1 equiv of H_2O_2, the formation of the 16-line spectrum is noted and the spectrum of **1a** has completely disappeared after 10 min (data not shown). The appearance of the broad signal is detectable in a slight asymmetry of the 16-line signal. These experiments show that the same reactivity is observed at low concentration of H_2O_2, but with a slower rate.

Figure 3 illustrates the EPR spectra recorded during the first second after adding H_2O_2 to an acetonitrile solution of **1a** using a rapid-mix freeze−quench apparatus. At 100 ms a 6-line spectrum is formed and coexists with that of **1a** (Figure 3b). This spectrum decays to the 16-line spectrum which starts appearing after 250 ms (data not shown) and has fully replaced the 6-line spectrum after ca. 500 ms (data not shown, see Figure 3c at 750 ms). At longer times (ca. 1−2 s, Figure 3d), the 16-line spectrum develops at the expense of that of **1a**. The 6-line spectrum is very similar to that observed in mononuclear Mn^{II} species. This clearly indicates that the first intermediate in the reaction of **1a** with H_2O_2 is an uncoupled Mn species (see below) which rapidly transforms into the one exhibiting the 16-line spectrum which dominates during the course of the reaction.

Influence of Acid and Base. Figure 4 illustrates the EPR spectra of **1a** in the presence of various quantities of added perchloric acid and triethylamine. Addition of 1 equiv of $HClO_4$ gives the spectrum of Figure 4a where a 6-line spectrum has appeared at the expense of the broad signal of **1a**, which is drastically reduced in intensity. Addition of a second equivalent of $HClO_4$ bleaches completely the spectrum of **1a** (Figure 4b) and the 6-line spectrum dominates, but the hyperfine coupling is now barely discernible owing to line broadening. Interestingly, adding 2 equiv of triethylamine (Figure 4c) regenerates the spectrum of **1a**. This indicates that the observed spectral changes are essentially due to protonation of **1a**. These experiments show that acid addition to **1a** gives rise to species in which the dinuclear

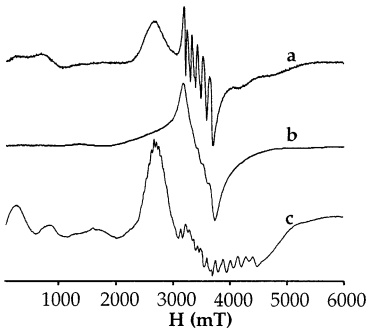

Figure 4. EPR spectra of **1a** in acetonitrile in the presence of $HClO_4$ and NEt_3: (a) **1a** + 1 equiv of $HClO_4$, (b) **1a** + 2 equiv of $HClO_4$, and (c) same as b + 2 equiv of NEt_3; reaction conditions, [**1a**] = 1.0 mM, T = 0 °C.

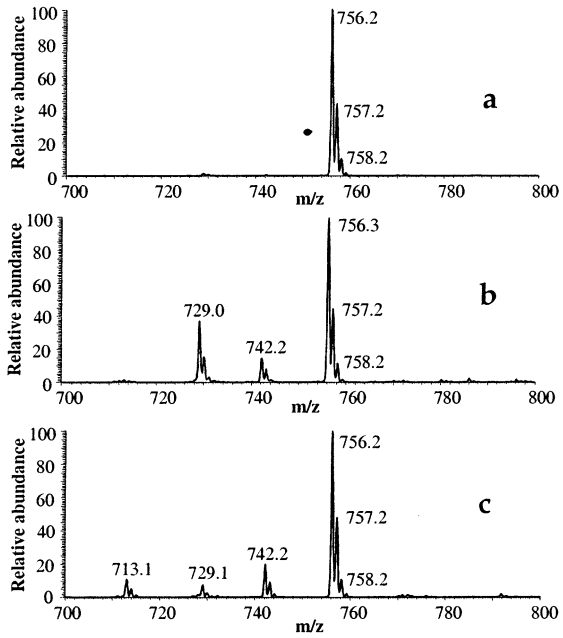

Figure 5. ESI-MS spectra of the reaction of **1a** with H_2O_2 in acetonitrile. Spectra a−c: reaction times 0, 5 min, and 40 min; reaction conditions, [**1a**] = 0.6 mM, [H_2O_2] = 460 mM, T = − 10 °C.

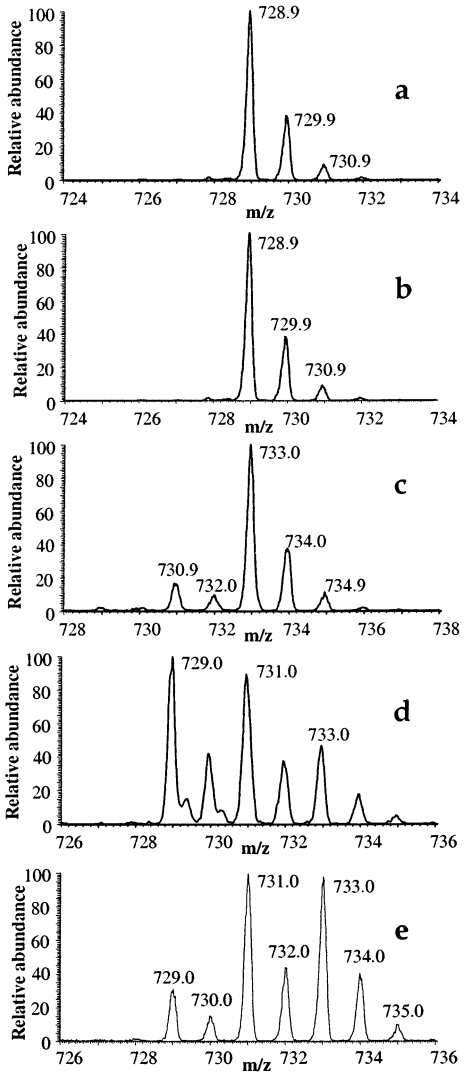

Figure 6. ESI-MS spectra of the reaction of **1a** with H_2O_2 and of **2a** in acetonitrile: (a) **1a** + 115 equiv of H_2O_2, (b) same as a + 200 equiv of $H_2{}^{18}O$, (c) **1a** + 40 equiv of $H_2{}^{18}O_2$ after 1 min, (d) = **1a** + 40 equiv of $H_2{}^{18}O_2$ after 30 min, and (e) **2a** + 50 equiv of $H_2{}^{18}O$; reaction conditions, [complex] = 0.6 mM, T = 20 °C.

unit is uncoupled and that this reaction is reversible. It is therefore likely that the protonation disrupts the phenoxo bridge, and probably also the acetate bridges, and that the phenol becomes protonated. Similar transformations have been observed in dicopper complexes of related phenol ligands.[28]

Mass Spectrometry. The disproportionation of H_2O_2 induced by **1a**,**b** was investigated by electrospray ionization mass spectrometry in two different ways. First, MS analysis was performed during the course of the reaction to identify the major species intervening at different times. Second, various isotopic labeling experiments were performed to get an insight into the mechanism of the reaction.

Figure 5 presents the positive mode ESI-MS spectra recorded before (a) and after (b, c) addition of H_2O_2 to an acetonitrile solution of **1a** at −10 °C. The spectrum of **1a** (Figure 6a) consists of a peak at m/z = 756 corresponding to the monocation $[Mn_2(L)(OAc)_2]^+$ obtained by loss of the coordinated solvent molecule. This peak persists throughout the reaction while the presence of **1a** is not detected in EPR under the same reaction conditions. This may arise from a highly preferential desorption of this species or, more likely, from its regeneration within the spectrometer. In this respect, it is worth noting that in positive ESI-MS **4a**, the dimanganese(II,III) analogue $\{[Mn_2(L)(OAc)_2]^{2+}$ of **1a**, is almost totally reduced to **1a**, while it is normally detected in the negative mode as the monoanion $\{[Mn_2(L)(OAc)_2](ClO_4)_3\}^-$. Figure 5b illustrates the ESI-MS spectrum recorded 5 min after addition of H_2O_2. Two new species have appeared with peaks at m/z = 729 and 742. The latter corresponds to the monocation $[Mn_2(L)(OAc)(HCO_2)]^+$ where one acetate group of **1a** has been replaced by a formate. The origin of the formate was traced to the methanol ligand and crystallization solvent of **1a**. This was clearly established by the observation that adding CD_3OD to the reaction mixture caused the peak at m/z = 742 to move to 743. This increase of 1 mass unit

(28) Belle, C.; Gautier-Luneau, I.; Pierre, J. L.; Le Pape, L.; Luneau, D. *Inorg. Chem.* **2000**, *39*, 3526−3636.

cannot be due to a protonation since adding D_2O (or H_2O in the presence of CD_3OD) has no effect and is therefore attributed to the formation of the DCO_2^- anion by oxidation of CD_3OD by H_2O_2 in the presence of **1a**. The peak at 729 (species **2a**) corresponds to the loss of an acetate bridge and the gain of two oxygen atoms. Two monocations can be envisaged with the corresponding mass: a dioxo dimanganese(III,IV) complex $[Mn_2(L)(OAc)(O)_2]^+$ and a peroxo dimanganese(II,III) complex $[Mn_2(L)(OAc)(O_2)]^+$. At times longer than 20 min, a new species (**3a**) appears (Figure 5c) characterized by a peak at $m/z = 713$. It has one less oxygen atom than the preceding one and is best formulated as an oxo dimanganese(II,III) species $[Mn_2(L)(OAc)(O)]^+$.

In the case of **1b**, the same species are detected with the corresponding changes in mass (+ 62 for a monocation) due to the replacement of an acetate by a benzoate: $m/z = 880$ $[Mn_2(L)(OBz)_2]^+$ **1b**, 804 $[Mn_2(L)(OBz)(HCO_2)]^+$, 791 $[Mn_2(L)(OBz)(O)_2]^+$ **2b**, and 775 $[Mn_2(L)(OBz)(O)]^+$ **3b**. This lends additional credence to the purported formula. It is worth noting that the formation of the latter two species, analogous to the intermediates **2a** and **3a**, respectively, is slower than in the case of **1a**.

The first series of isotopic labeling experiments was designed to definitely probe the structure of the $m/z = 729$ intermediate since the mass itself could not distinguish between the peroxo dimanganese(II,III) and the dioxo dimanganese(III,IV) formulations. We reasoned that if the latter formulation is the correct one, we should observe the exchange of the two oxo oxygens with ^{18}O-labeled water giving a mass increase of 4 mass units. Indeed such an exchange has been evidenced by vibrational spectroscopies,[29,30] The results of these experiments are illustrated in Figure 6. Figure 6b shows the isotopic pattern of the 729 ion in the reaction mixture obtained ca. 2 min after H_2O_2 is reacted with **1a** in the presence of $H_2{}^{18}O$. It is indistinguishable with the one of Figure 6a recorded in the absence of $H_2{}^{18}O$ (but with an equivalent amount of H_2O) and points therefore to the absence of labeling. Figure 6c shows the isotopic pattern of the **2a** ion in the reaction mixture obtained 1 min after addition of 40 equiv of $H_2{}^{18}O_2$ to **1a**. This spectrum shows a pattern of peaks at 733, in agreement with the incorporation of two ^{18}O atoms in **2a**. The low-intensity peak at 731 corresponds to a ca. 10% amount of $H_2{}^{16}O{}^{18}O$ in the $H_2{}^{18}O_2$ reagent. Both experiments concur to show that the two O atoms of **2a** come from H_2O_2 and do not exchange with water under these conditions. Nevertheless, when the same reaction mixture **1a**/$H_2{}^{18}O_2$ is analyzed at longer times (ca. 30 min vs 1 min) the spectrum of Figure 6d is obtained. It shows that the pattern of unlabeled **2a** at 729 has been re-formed and coexists with patterns at 731 and 733 corresponding respectively to singly and doubly labeled **2a**. The presence of the singly labeled species shows that the two O atoms are exchanged independently, which is inconsistent with the peroxo dimanganese(II,III) formulation. These observations can be explained by taking into account that the rate of the oxo exchange (see below) is about 2 orders of magnitude slower than that of the H_2O_2 disproportionation.[31] Therefore, at the beginning of the reaction when the concentration of H_2O_2 is large, the disproportionation reaction dominates and the two O atoms of **2a** come from H_2O_2, but when the reaction slows down by lack of H_2O_2, the oxo exchange becomes competitive and these oxo ligands are "back-exchanged" by the unlabeled water present in the reaction mixture. The fact that the labeling of the oxo ligands does not occur in the early stages of the reaction but only when most of H_2O_2 has been consumed indicates that **2a** indeed belongs to the catalytic cycle. Identical observations were made in the case of **1b**.

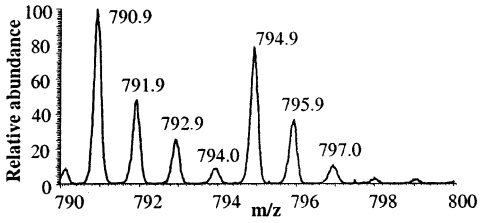

Figure 7. ESI-MS spectra of the reaction of **1b** with an equimolar mixture of H_2O_2 and $H_2{}^{18}O_2$ in acetonitrile. Reaction conditions: [**1b**] = 0.6 mM, T = 20 °C; $[H_2{}^{16}O_2] = [H_2{}^{18}O_2]$ = 12 mM.

Having seen that the two O atoms come from H_2O_2, the question now is: do they come from a single or from two different H_2O_2 molecules? To answer this question, we reacted **1** with an approximately equimolar mixture of H_2O_2 and $H_2{}^{18}O_2$. Both **1a** and **1b** reacted in the same way. Here we present the results obtained with **1b** because they are less disturbed by the oxo back-exchange because **1b** reacts more slowly than **1a**. As noted above, **2b**, the benzoate analogue of **2a**, exhibits a peak at $m/z = 791$. If the two O atoms come from the same H_2O_2 molecule, one expects to observe under our conditions two equally intense peaks at 791 and 795, while three peaks in the ratio 1:2:1 are expected at $m/z = 791$, 793, and 795 if the O oxygens come from different H_2O_2 molecules. Figure 7, which illustrates the ESI-MS of the reaction mixture, clearly indicates that the former case is observed, therefore demonstrating that the two O atoms come from a single H_2O_2 molecule.

Synthesis and Characterization of the Dioxodimanganese(III,IV) Intermediate. Synthesis. EPR spectroscopy and electrospray mass spectrometry (ESI-MS) show that the dioxodimanganese(III,IV) complexes of the ligand HL with the formula $[Mn_2(L)(O)_2(OX)]^+$ (X = Ac or Bz) constitute active species in the disproportionation of H_2O_2 induced by its dimanganese(II,II) derivatives. Since the positive identification of a catalyst in this reaction is rather rare, we decided to prepare it independently and to characterize both its structure and its properties.

Since these compounds are formed, but unstable, in the presence of H_2O_2, we reasoned that they should be obtained by using *tert*-butyl hydroperoxide (TBHP), which is as powerful an oxidizing agent as H_2O_2 but cannot be as easily

(29) Cooper, S.; Calvin, M. *J. Am. Chem. Soc.* **1977**, *99*, 6623−6630.
(30) Dave, B. C.; Czernuszewicz, R. S. *Inorg. Chim. Acta* **1994**, *227*, 33−41.
(31) Dubois, L.; Tan, X. S.; Xiang, D. F.; Latour, J. M. Manuscript in preparation.

oxidized. Indeed, Pecoraro et al.[32] reported that reaction of this reagent with a dimanganese(III) complex afforded the dimanganese(III,IV) derivative in the case of alcoholate complexes. Reaction of the dimanganese(II) complex $[Mn_2(L)(OAc)_2](ClO_4)$ **1a** with 1.5 equiv of TBHP in acetonitrile affords almost quantitatively the desired complex **2a** $[Mn_2(L)(O)_2(OAc)]^+$, but traces of **1a** could still be detected by EPR spectroscopy and ESI-MS. A systematic study of the stoichiometry of both reagents revealed that the use of 7 equiv of TBHP affords a rapid (10−15 min) and clean formation of the $Mn^{III}Mn^{IV}$ species, as judged by EPR and ESI-MS. It is worth noting that these EPR and UV−visible spectra were identical with those recorded during the catalysis.

The dimanganese(III,IV) complex is not stable at room temperature even in the presence of an excess of TBHP (see below). Indeed, under these conditions decomposition to unidentified manganese(II) species is observed within a couple of minutes as shown by the bleaching of the solution. Lowering the temperature to −20 °C brings sufficient stability to perform spectroscopic and analytical measurements but not to crystallize the compound.

Mass Spectrometry Analysis. ESI-MS was used to assign unambiguously the nature of the oxo ligands through the use of labeling experiments. The ESI-MS spectrum of **2a** recorded in the reaction mixture is identical to that depicted in Figure 6a. The peak at $m/z = 729$ corresponds to the mass expected for the cation $[Mn_2(L)(O)_2(OAc)]^+$. When labeled water $H_2{}^{18}O$ is added to the reaction mixture, the ESI-MS spectrum presents two prominent peaks at $m/z = 733$ and 731 while that at 729 is drastically reduced in intensity (Figure 6e). This demonstrates that **2a** contains two oxo ligands which have been exchanged independently. The incomplete labeling is due to the presence of unlabeled water as TBHP solvent. It is worth noting that a monitoring of the oxo ligand exchange showed that the half-time of the reaction is ca. 1 min.

UV−Visible Spectroscopy. In acetonitrile solution, the electronic absorption spectrum of **2a** possesses three poorly resolved absorptions or shoulders at 630, 550, and 460 nm with respective molar extinction coefficients of 900, 1200, and 2900 $M^{-1}\cdot cm^{-1}$. These three absorptions are characteristic of dioxodimanganese(III,IV) complexes. These spectra have been thoroughly studied by Solomon et al.[27] According to their analysis, the absorptions at higher and lower energies can be assigned to oxo to Mn charge transfer transitions while that at intermediate energy is a d−d transition. Nevertheless, it is worth noting that **2a** exhibits more intense absorptions than similar complexes of tripodal amine ligands.[17,33−35] Indeed, the extinction coefficients of **2a** are ca. twice those of these complexes for their three absorption bands: 2900 vs 1000−1300 $L\cdot mol^{-1}\cdot cm^{-1}$ at ∼430 nm, 1200 vs 400−600 $L\cdot mol^{-1}\cdot cm^{-1}$ at ∼550 nm, and 900 vs 400−600 $L\cdot mol^{-1}\cdot cm^{-1}$ at ∼650 nm. The origin of this specific feature may be found in an underlying charge transfer transition of the phenoxo ligand to the Mn^{III} and/or Mn^{IV} ion (see below).

Table 1

tensor axes	g	$\lvert A_1\rvert$[d] 10^{-4} cm^{-1}	$\lvert A_2\rvert$ 10^{-4} cm^{-1}	δB[a] mT	R[b]
X	2.0021	138 (140)	76	1.0	0.02
Y	2.0018	154 (157)	70		
Z	1.987	99 (99)	75		
isotropic value[c]	1.997	130 (131)	74		

[a] Spectral bandwidth (half-width at half-height). [b] Agreement factor: $R = \sum_i(I_i^{exp} - I_i^{calc})^2/\sum_i(I_i^{exp})^2$. [c] $A_{iso} = (A_x + A_y + A_z)/3$. [d] Values in parentheses refer to the complex $[Mn^{III}Mn^{IV}(O)_2(OAc)(tacn)_2](BPh_4)_2$.[37,51]

EPR Spectroscopy. 2a exhibits an EPR spectrum (Figure 2e) which is a 16-line spectrum characteristic of $Mn^{III}Mn^{IV}$ species.[36,37] It results from an electronic spin doublet in strong interaction with the two $I = {}^5/_2$ nuclear spins of the ^{55}Mn ions. This spectrum was successfully simulated (Figure 2f) using the parameters listed in Table 1. Looking at the hyperfine tensors, ion 1 can be safely assigned to Mn^{III} for two reasons: (i) the isotropic value is approximately twice that for the other ion and (ii) the tensor is strongly anisotropic; the component along the z axis is smaller than the two other ones, which is consistent with the presence of the Jahn−Teller effect of Mn^{III}.

Extended X-ray Absorption Fine Structure (EXAFS). Owing to the instability of **2a**, we investigated its structure through X-ray absorption measurements with the help of two model dioxodimanganese(III,IV) compounds whose structure is known from crystallography: $[Mn_2(O)_2(OAc)(bpea)_2](PF_6)_2$,[17] **5**, and $[Mn_2(O)_2(tpa)_2](ClO_4)_3$,[18] **6**, obtained with the ligands bispicolylethylamine (bpea) and trispicolylamine (tpa), respectively. These two compounds differ structurally in the fact that in **5** a bridging acetate caps the Mn_2O_2 core.

Figure 8 illustrates the Fourier transform of the two model compounds, **5** (top) and **6** (middle), and of **2a** (bottom). The FTs of the model compounds present two main peaks (dashed lines). The first one corresponds to the short Mn−(μ)O distance at ca. 1.80 Å while the second one corresponds to the Mn−Mn distance at ca. 2.65 Å. Between these two peaks, peak(s) corresponding to the Mn−N interaction is (are) present. The fits of the model compounds reproduce well the different crystallographic Mn−O and Mn−Mn distances (Table 2). Concerning the Mn−N shells, the distance spread is large and destructive interferences are likely to be present.

For **2a**, two statistically equivalent fits have been obtained (Table 2). They differ by the distribution of atoms within the first two shells: either two or three O atoms at a short distance (1.87 Å) and three or two N/O atoms at a longer distance (2.14 Å). In addition one N atom is found at a longer

(32) Caudle, M. T.; Riggs-Gelasco, P.; Gelasco, A. K.; Penner-Hahn, J. E.; Pecoraro, V. L. *Inorg. Chem.* **1996**, *35*, 3577−3584.
(33) Hagen, K. S.; Armstrong, W. H.; Hope, H. *Inorg. Chem.* **1988**, *27*, 967−969.
(34) Goodson, P. A.; Glerup, J.; Hodgson, D. J.; Michelsen, K.; Pedersen, E. *Inorg. Chem.* **1990**, *29*, 503−508.
(35) Horner, O.; Charlot, M. F.; Boussac, A.; Anxolabéhère-Mallart, E.; Tchertanov, L.; Guilhem, J.; Girerd, J. J. *Eur. J. Inorg. Chem.* **1998**, 721−727.
(36) Zheng, M.; Khangulov, S. V.; Dismukes, G. C.; Barynin, V. V. *Inorg. Chem.* **1994**, *33*, 382−387.
(37) Schäfer, K. O.; Bittl, R.; Zweygart, W.; Lendzian, F.; Haselhorst, G.; Weyermüller, T.; Wieghardt, K.; Lubitz, W. *J. Am. Chem. Soc.* **1998**, *120*, 13104−13120.

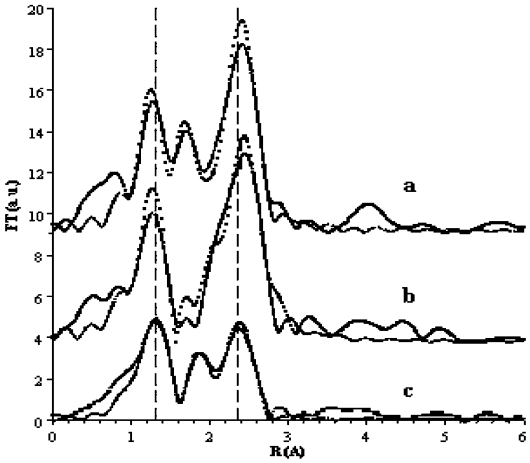

Figure 8. Fourier transform of **2a** and reference complexes: (a) $[Mn_2(O)_2(OAc)(bpea)_2](PF_6)_2$ **5**, (b) $[Mn_2(O)_2(tpa)_2](ClO_4)_3$ **6**, and (c) **2a**. The dots are the experimental spectra and the solid lines the simulations.

Table 2

N	*R* (Å)	σ^2 ($\times 10^3$ Å^2)	N_{diffr}	R_{diffr} (Å)
2a				
2 O	1.86(2)	8.4(4)		
3 N	2.14(2)	11.3(7)		
1 N	2.32(2)	3.9(3)		
1 Mn	2.63(2)	9.8(5)		
or				
3 O	1.88(2)	12.5(7)		
2 N	2.14(2)	4.2(3)		
2 N	2.31(2)	4.8(4)		
1 Mn	2.62(2)	9.2(5)		
$[Mn_2(O)_2(tpa)_2](ClO_4)_3$				
2 O	1.82(2)	4.9(3)	2 O	*1.81*
3 N	2.06(2)	5.7(5)	3 N	*2.05*
2 N	2.28(2)	3.3(3)	1 N	*2.24*
1 Mn	2.69(2)	3.5(4)	1 Mn	*2.64*
$[Mn_2(O)_2(OAc)(bpea)_2](PF_6)_2$				
2 O	1.81(2)	5.4(4)	2 O	*1.82*
3 N	2.08(2)	4.6(3)	1 N	*1.94*
2 N	2.28(2)	5.1(4)	3 N	*2.09*
1 Mn	2.65(2)	3.8(3)	1 N	*2.31*
			1 Mn	*2.63*

distance (2.3 Å) and one Mn at 2.63 Å. The Debye−Waller factors of these shells are relatively large, especially for the first two shells. This is likely due to the different oxidation states and environments of the two Mn atoms provided by the phenolate ligand (see below) which result in a distance distribution and the fact that the $Mn-O_{phenoxo}$ and $Mn-O_{carboxylato}$ bond distances are intermediate between the $Mn-O_{oxo}$ and $Mn-N_{pyridine}$ distances. The short Mn−O distance is longer than the $Mn-O_{oxo}$ bond lengths of the two model compounds while the Mn−Mn distance is comparable to that of **6** as can be seen in Figure 8.

Electrochemical Behavior. The redox behavior of **2a** has been investigated at −20 °C in acetonitrile (10^{-1}M tetrabutylammonium perchlorate). In oxidation (Figure S4, Supporting Information), a reversible wave is observed at $E_{1/2}$ = 0.91 V_{NHE} ($\Delta E_{1/2}$ = 0.08 V). Exhaustive electrolysis at 0.98 V_{NHE} consumes 0.83 electron per dinuclear complex, in agreement with a one-electron transfer, and yields about

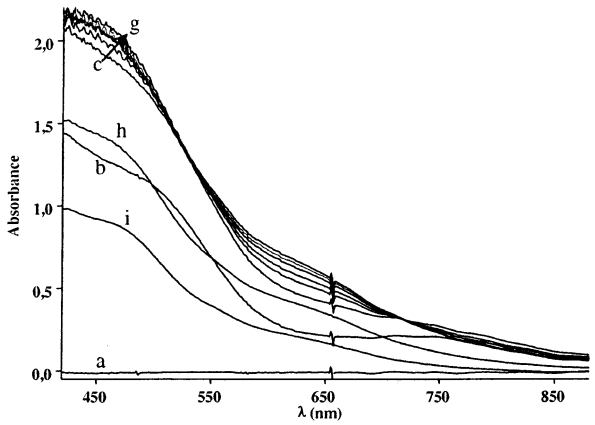

Figure 9. UV−visible monitoring of the reaction of **1a** with TBHP in acetonitrile. Reaction times a−i: 0, 60, 120, 180, 240, 300, 360, 420, and 1200 s; reaction conditions, [**1a**] = 1 mM, [TBHP] = 7 mM, T = − 10 °C.

80% of the oxidized species. This oxidation can therefore be assigned to the $Mn^{III}Mn^{IV}/Mn^{IV}Mn^{IV}$ couple.

In reduction (Figure S4, Supporting Information), two irreversible waves are noted at −0.18 and −0.29 V_{NHE}. Exhaustive electrolysis at − 0.4 V_{NHE} consumes 2.3 electrons per dinuclear complex. The CV of the reduced solution shows a broad oxidation peak at 1.1 V_{NHE} associated with a shoulder at 0.7 V_{NHE}. This suggests that the $Mn^{III}Mn^{III}$ species derived from **2a** is unstable as already observed for other dioxo $Mn_2^{III,IV}$ complexes.[20,38,39] On the other hand the resulting solution does not still exhibit the typical absorption band of the di-μ−oxo species at 460 nm. This indicates that the reduction of **2a** involves probably the breaking of the oxo bridges and leads to some unidentified manganese(II) complexes.

Mechanism of Formation of 2a. UV−Visible Spectroscopy. The reaction of TBHP with **1a** was monitored by UV−visible and X-ray absorption spectroscopies in order to get an insight into the mechanism of formation of the $Mn^{III}Mn^{IV}$ complex and possibly into the mechanism of the H_2O_2 disproportionation reaction.

Figure 9 shows the time dependence of the electronic absorption spectrum of an acetonitrile solution of **1a** (Figure 9a) after addition of TBHP at −10 °C. Three phases can be distinguished. In the first one (ca. 120 s, Figure 9c) an intermediate accumulates with main absorptions at 750 and 500 nm. Then, this intermediate transforms into **2a** characterized by the three absorptions at 630, 550, and 460 nm. This transformation occurs with an isosbestic point at 720 nm, which indicates that it does not involve any other intermediate (Figures 9c−g). After accumulating for ca. 6 min, **2a** starts to decompose to Mn^{II} species as seen by the continuous loss of absorbance without new absorptions appearing (Figure 9h,i). These experiments definitely show that the formation of **2a** occurs through an intermediate which exhibits moderately intense absorptions in the 400−800 nm domain.

(38) Mahapatra, S.; Das, P.; Mukherjee, R. *J. Chem. Soc., Dalton Trans.* **1993**, 217−220.
(39) Lal, T. K.; Mukherjee, R. *Inorg. Chem.* **1998**, *37*, 2373−2382.

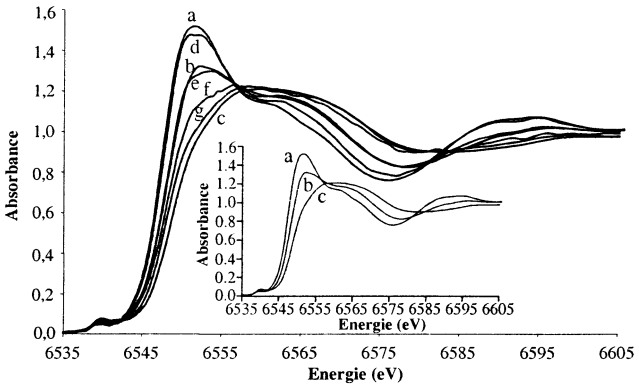

Figure 10. Comparison of the XANES spectra of the reaction of **1a** with TBHP in toluene/acetonitrile with those of **1a**, **2a**, and **4a**. Spectra a−c and inset: **1a**, **4a**, and **2a**. Spectra d−g: reaction times 10, 120, 240, and 420 s; reaction conditions, [**1a**] = 1 mM, [TBHP] = 7 mM, $T = -10$ °C.

X-ray Absorption Spectroscopy. In order to validate this kinetics and obtain structural information on the intermediate, the reaction of **1a** with TBHP was followed by X-ray absorption spectroscopy at the Mn edge. The inset of Figure 10 presents the XANES of **1a** (spectrum a), its $Mn^{II}Mn^{III}$ analogue[16] **4a** (spectrum b), and **2a** (spectrum c), which differ by the oxidation state of the dimanganese center: $Mn^{II}Mn^{II}$, $Mn^{II}Mn^{III}$, and $Mn^{III}Mn^{IV}$, respectively. A significant evolution of the edge energy is observed from 6546.6 for **1a** to 6547.7 for **4a** and 6548.9 for **2a**. This shift is consistent with the analyses made by Wieghardt et al.[40] and Yachandra et al.,[41] who estimated to ca. 1 eV the shift induced by oxidation of the dimanganese center by 1 unit. A significant change of the shape of the edge peak is noted also, especially in the case of **2a**, which reflects the structural change of the Mn coordination spheres. Figure 10 shows the XANES spectra recorded after freezing of the reaction mixture at various times after TBHP addition, superimposed on the spectra of **1a**, **4a**, and **2a**. After 10 s (spectrum d), the reaction has not progressed much and the XANES spectrum strongly resembles that of **1a**. After 2 min, the XANES spectrum of the reaction mixture (spectrum e) is almost superimposable to that of **4a**, and this match extends beyond the edge region. After 7 min, the spectrum of the mixture (spectrum g) is very close to that of **2a**, and again this extends to higher energy. These experiments are perfectly consistent with those using electronic absorption spectroscopy since they point to the formation of an intermediate in the same time period and, moreover, they show that this intermediate is a $Mn^{II}Mn^{III}$ species very similar to **4a**.

Discussion

Our spectroscopic monitoring of the disproportionation of H_2O_2 induced by **1a**,**b** has shown that both compounds react in the same way and that **1a** reacts significantly faster than **1b**. During the course of these studies, three intermediates have been detected. The dimanganese(III,IV) complexes **2** appear early and dominate during the reaction while the dimanganese(II,III) species **3** can be detected only in the second part of the reaction. Freeze−quench experiments have shown that another intermediate **7** is formed in the very early stages of the reaction and precedes the formation of **2**. In the following, we will discuss the possible structures of these species and the mechanism of H_2O_2 reduction.

Dioxodimanganese(III,IV) Species 2. The dimanganese complex **2a** is obtained by reaction of the dimanganese(II,II) complex **1a** with *tert*-butyl hydroperoxide. EPR spectroscopy shows that it is the species involved in the catalytic disproportionation of hydrogen peroxide by **1a**. Indeed, quantitation of the signal recorded during the reaction (Figure 2b) with respect to that of as isolated **2a** shows that it corresponds to ca. 70% of the dimanganese species, while not more than 10% of **1a** is still present. Owing to the presence of dioxygen bubbles trapped when freezing the EPR tube, these percentages are approximate, but the order of magnitude is reliable. As the catalytic reaction progresses, the quantity of **2a** decreases to ca. 20% after 10 min (Figure 2c) and ca. 5% after 50 min (Figure 2d) owing to the continuous accumulation of **3a**. Labeling experiments coupled to mass spectrometry have shown unambiguously that **2a** contains two oxo ligands. UV−visible and EPR spectroscopies have revealed that it possesses the characteristic features of dioxodimanganese(III,IV) species. Moreover, the presence of this Mn_2O_2 core has been definitely established by X-ray absorption spectroscopy. All accumulated physical data point to a strong similarity of **2a** with the usual dioxo $Mn^{III}Mn^{IV}$ complexes derived from polyamine ligands. How is it possible to accommodate the Mn_2O_2 core within the hexadentate phenolate ligand, or, in other words, what is the binding mode of the phenolate in **2a**, and does the dimanganese unit retain a carboxylate bridge? ESI-MS experiments indicate that the phenol ligand is deprotonated. Moreover, as noted earlier, the extinction coefficients of the absorption bands of **2a** in the visible region exceed those of the polyamine complexes.[33−35] This is an indication that phenolate to Mn charge transfer transitions operate and therefore that the phenolate is bound to at least one manganese ion. Can it be bridging? Structural studies have shown that capping the Mn_2O_2 core by an additional carboxylate shortens the intermanganese distance.[17] Examination of the literature reveals that the latter spans the range 2.64−2.74 Å in the unsupported dioxo complexes[18,30,33,34,37,42−45] while in the carboxylate-capped systems it is confined to the 2.59−2.67 Å domain.[17,37−39,46−51] Our EXAFS studies have shown that

(40) Bossek, U.; Hummel, H.; Weyhermuller, T.; Wieghardt, K.; Russell, S.; Wolf, L. v. d.; Kolb, U. *Angew. Chem., Int. Ed. Engl.* **1996**, *35*, 1552−1554.
(41) Visser, H.; Anxolabéhère-Mallart, E.; Bergmann, U.; Glatzel, P.; Robblee, J. H.; Cramer, S.; Girerd, J.-J.; Sauer, K.; Klein, M. P.; Yachandra, V. K. *J. Am. Chem. Soc.* **2001**, *123*, 7031−7039.
(42) Plaksin, P. M.; Stoufer, R. C.; Mathew, M.; Palenik, G. J. *J. Am. Chem. Soc.* **1972**, *94*, 2121−2122.
(43) Stebler, M.; Ludi, A.; Burgi, H.-B. *Inorg. Chem.* **1986**, *25*, 4743−4750.
(44) Brewer, K.; Calvin, M.; Lumpkin, R. S.; Otvos, J. W.; Spreer, L. O. *Inorg. Chem.* **1989**, *28*, 4446−4451.
(45) Goodson, P.; Hodgson, D. J. *Inorg. Chim. Acta* **1990**, *172*, 49−57.
(46) Wieghardt, K.; Bossek, U.; Zsolnai, L.; Huttner, G.; Blondin, G.; Girerd, J. J.; Babonneau, F. *J. Chem. Soc., Chem. Commun.* **1987**, 651−3.
(47) Bashkin, J. S.; Schake, A. R.; Vincent, J. B.; Chang, H. R.; Li, Q.; Huffman, J. C.; Christou, G.; Hendrickson, D. N. *J. Chem. Soc., Chem. Commun.* **1988**, 700−701.

the intermanganese distance in **2a** (2.63 Å) is slightly shorter than those of the unsupported dioxo complexes (2.69 Å in **6**) and similar to those of the carboxylate-capped cores (2.65 Å in **5**). Such a shortening is smaller than reasonably expected for the introduction of a third single atom bridge. Indeed, this distance can become as short as ca. 2.3 Å in (tris-μ-oxo)dimanganese(IV) species.[52] Therefore we are led to the conclusion that the phenolate in **2a** is certainly coordinated but not bridging. On the other hand, the Mn−Mn distance is consistent with the presence of a carboxylato-capped oxodimanganese(III,IV) species but only marginally outside the domain of the unsupported core. Nevertheless, it cannot be excluded that the rather short Mn−Mn distance may result in **2a** from constraints imposed by the binucleating phenolate ligand. Therefore Mn−Mn distance alone does not prove unambiguously the presence of a carboxylate bridge.

The effect of capping the Mn_2O_2 core by a carboxylate has been shown in most cases to modify significantly the intensity pattern of the 16-line EPR spectrum.[37] A similar or even stronger effect would be expected for a phenolate-capped system, and therefore such a system is not likely. On the other hand, both the shape of the spectrum and the parameters derived therefrom match almost perfectly those of the dioxo- and acetato-bridged tacn complex $[Mn^{III}Mn^{IV}(O)_2(OAc)(tacn)_2](BPh_4)_2$[37,51] (tacn = triazacyclononane, see Table 1). Accordingly both the EPR and the structural results seem to indicate that **2a** is a carboxylato-bridged dioxo dimanganese(III,IV) species (Scheme 2).

Comparing the electronic absorption properties of **2a** to literature data brings some clues to its binding mode to the Mn_2O_2 core. A few dimanganese(III,IV) phenolate complexes have been described.[53,54] They possess very intense phenolate to Mn^{IV} charge transfer transitions in the visible region similar to those observed in mononuclear phenolate Mn^{IV} complexes.[55] By contrast, phenolate to Mn^{III} charge transfer transitions occur at higher energy with a smaller intensity.[56−58] In this respect, it is worth noting that the dimanganese(II,III) complex **4a** presents three absorptions at 380, 485, and 627 nm with respective extinction coefficients 1270, 960, and 680 cm^{-1} M^{-1}.[16] Therefore the presence of an underlying phenolate to Mn^{III} charge transfer transition can explain the enhanced absorptions of **2a** with respect to usual dioxo $Mn^{III}Mn^{IV}$ complexes, and this suggests that in **2a** the phenolate is bound to the Mn^{III} ion. The electrochemical study which shows that the potential of the $Mn^{III}Mn^{IV}/Mn^{IV}Mn^{IV}$ couple is ca. 250 mV less positive in **2a** than in complexes of polyamine ligands[17,18,38] is consistent with this view.

Oxodimanganese(II,III) Species 3. ESI-MS monitoring allowed a dimanganese(II,III) species to be detected in late stages of the disproportionation reaction and showed that it is derived from H_2O_2 and is catalytically competent. The characteristics of the EPR signal associated with this species are consistent with a dimanganese(II,III) formulation. In particular, the envelope around $g = 2$ which extends over ca. 2000 G and outflanks the 16-line signal is reminiscent of the signals observed for (μ-phenoxo)Mn(II)Mn(III) complexes.[16,36,59] This species has been identified by ESI-MS, and the corresponding cation can be formulated as $[Mn_2(L)(OAc)(O)]^+$. Two structures can be envisaged for this cation depending on the binding mode, bridging or terminal, of the oxo ligand. To the best of our knowledge, there is no report of a stable μ-oxo dimanganese(II,III) compound. Such a species can be formed electrochemically from the well-known μ-oxo-bis-μ-acetato dimanganese(III,III) complexes,[20,38] but it decomposes to Mn^{II} species. On the other hand, a Mn complex with a terminal oxo ligand has been described recently.[60] At first sight, the oxo-bridged structure should be favored on the basis that its interconversion with **2** would require a minimal rearrangement. Nevertheless, since the two oxygens of **2** originate from the same molecule of H_2O_2, this argument does not hold. On the contrary, substitution of the terminal oxo ligand on Mn^{III} by a peroxide ligand would be feasible since this reaction has precedents in the inorganic literature.[61,62]

Intermediate 7. The rapid-mix freeze−quench experiments coupled to EPR have revealed the formation of a short-lived species **7** in the range 100−500 ms. It is characterized by a 6-line spectrum (Figure 4c) which coexists with that of **1a** and decays rapidly to that of **2a**. Interestingly, an almost superimposable spectrum is obtained upon treating **1a** with 1 equiv of $HClO_4$ (Figure 4a). The resulting spectrum is different from the one obtained upon dissolving $Mn(H_2O)_6(ClO_4)_2$ in acetonitrile, which shows that the Mn ions are still coordinated to the ligand. As noted above, it is likely that in such a species the protonation has induced the disruption of the phenoxo bridge giving rise to a 6-line EPR spectrum as observed in mononuclear Mn^{II} species. A similar

(48) Bossek, U.; Saher, M.; Weyermüller, T.; Wieghardt, K. *J. Chem. Soc., Chem. Commun.* **1992**, 1780−1781.
(49) Pal, S.; Gohdes, J. W.; Wilisch, W. C. A.; Armstrong, W. H. *Inorg. Chem.* **1992**, *31*, 713−716.
(50) Mok, H. J.; Davis, J. A.; Pal, S.; Mandal, S. K.; Armstrong, W. H. *Inorg. Chim. Acta* **1997**, *263*, 385−394.
(51) Zweygart, W.; Bittl, R.; Wieghardt, K.; Lubitz, W. *Chem. Phys. Lett.* **1996**, *261*, 272−276.
(52) Wieghardt, K.; Bossek, U.; Nuber, B.; Weiss, J.; Bonvoisin, J.; Corbella, M.; Vitols, S. E.; Girerd, J. J. *J. Am. Chem. Soc.* **1988**, *110*, 7398−7411.
(53) Baldwin, M. J.; Stemmler, T. L.; Riggs-Gelasco, P. J.; Kirk, M. L.; Penner-Hahn, J. E.; Pecoraro, V. L. *J. Am. Chem. Soc.* **1994**, *116*, 11349−11356.
(54) Horner, O.; Anxolabéhère-Mallart, E.; Charlot, M. F.; Tchertanov, L.; Guilhem, J.; Mattioli, T. A.; Boussac, A.; Girerd, J. J. *Inorg. Chem.* **1999**, *38*, 1222−1232.
(55) Auerbach, U.; Weyermüller, T.; Wieghardt, K.; Nuber, B.; Bill, E.; Butzlaff, C.; Trautwein, A. X. *Inorg. Chem.* **1993**, *32*, 508−519.
(56) Patch, M. G.; Simolo, K. P.; Carrano, C. J. *Inorg. Chem.* **1982**, *21*, 2972−2977.
(57) Neves, A.; Erthal, S. M. D.; Vencato, I.; Ceccato, A. S.; Mascarehas, Y. P.; Nascimento, O. R.; Hörner, M.; Batista, A. A. *Inorg. Chem.* **1992**, *31*, 4749−4755.
(58) Shongwe, M. S.; Mikuriya, M.; Nukada, R.; Ainscough, E. W.; Brodie, A. M.; Waters, J. M. *Inorg. Chim. Acta* **1999**, *290*, 228−236.
(59) Diril, H.; Chang, H.; Nilges, M.; Zhang, X.; Potenza, J.; Schugar, H.; Isied, S.; Hendrickson, D. *J. Am. Chem. Soc.* **1989**, *111*, 5102−5114.
(60) Shirin, Z.; Hammes, B. S.; V G Young, J.; Borovik, A. S. *J. Am. Chem. Soc.* **2000**, *122*, 1836−1837.
(61) Latour, J. M.; Galland, B.; Marchon, J. C. *J. Chem. Soc., Chem. Commun.* **1979**, 570−571.
(62) Bortolini, O.; DiFuria, F.; Modena, G. *J. Am. Chem. Soc.* **1981**, *103*, 3924−3926.

chemistry is observed for dicopper complexes of related phenolate ligands.[28]

Moreover, the same 6-line spectrum fully develops upon addition of 1 equiv of $HClO_4$ to **4a** (data not shown) while 2 equiv is necessary to fully transform **1a**. This difference can be understood on the basis of the respective structures of **1a** and **4a**. Indeed, the structural characterization of **1a** and **4a** has shown that the $Mn^{II}-O_{phenoxo}$ bond is significantly elongated and weakened in the latter,[16] which makes the phenol oxygen more susceptible to protonation in the mixed-valent compound. This may indicate that an oxidation of one Mn of the pair occurs with the protonation and therefore that the observed species is the protonated $Mn^{II}Mn^{III}$ phenolate complex. Support for an initial one-electron oxidation of **1a** is afforded by the XANES study of its reaction with TBHP. A protonated and uncoupled $Mn^{II}Mn^{III}$ species appears therefore a likely intermediate to produce the catalytically active $Mn^{III}Mn^{IV}$ and enter the catalytic cycle.

Mechanism of the Reduction of H_2O_2 by 1a,b. ^{18}O labeling experiments have provided mechanistic information on H_2O_2 reduction in the present system. Indeed, the experiments involving unlabeled and doubly labeled H_2O_2 have shown that the labels are not scrambled in the resulting dioxodimanganese(III,IV) species. This shows that the two oxygens of the Mn_2O_2 core come from a single molecule of H_2O_2 and therefore that both oxygens of the peroxide adduct must bind to the Mn ions. In other words, this demonstrates the occurrence of a $\mu_{1,2}$ bridging mode of the peroxide. The $\mu_{1,2}$-peroxo and η^2-$\mu_{1,2}$-peroxo bridging modes appear the most plausible candidates, but there is no element to favor any one of them at the moment, although a η^2-$\mu_{1,2}$-peroxo would more easily give the dioxodimanganese(III,IV) core. Inversely, any $\mu_{1,1}$-hydroperoxo bridging mode is ruled out by these experiments.

Having discussed the most plausible structures of the various intermediates, we can try and envisage how they could operate. The catalase-like reaction shuttles between **2** and **3**. Let us consider the reduction of H_2O_2 by **3**. If **3** is a μ-oxo species, the oxo bridge must be substituted by the incoming peroxide to give a μ-peroxo species which will eventually rearrange into the dioxo complex **2**. Two $\mu_{1,2}$-peroxodimanganese species have been described in the literature.[63,64] More interestingly, if **3** is an oxo Mn^{III} species, a different chemistry can take place. Indeed, it has been shown for several oxo metal complexes that a terminal oxo group can be easily substituted by a peroxo group with water elimination.[61,62] Such a process would give rise to a side-on η^2-peroxo Mn^{III} complex, two examples of which have been reported in the literature.[65,66] This peroxo complex would then be reduced by the neighboring Mn^{II} ion to give **2**.

Summary and Biological Relevance

The present study is one of the rare examples where active species involved in H_2O_2 disproportionation by phenolato dimanganese complexes have been identified. These are an oxodimanganese(II,III) and a dioxodimanganese(III,IV) complex, respectively, the reduced and the oxidized states between which the reaction shuttles. These species bear some resemblance with the manganese catalase active site, in particular the likely occurrence of a Mn_2O_2 core. Of course, they do not function at the same oxidation state as the enzymes, since the latter operate between the $Mn^{II}Mn^{II}$ and the $Mn^{III}Mn^{III}$ states.[7] Labeling studies have established that they are indeed involved in the catalysis, and moreover they have established how they are formed. In this respect, it is important to note that the two oxygen atoms of the dioxodimanganese core of the oxidized form come from the same peroxide molecule. An analogous observation was made earlier by Pecoraro et al. when they studied H_2O_2 disproportionation by $Mn^{III}Mn^{III}/Mn^{IV}Mn^{IV}$ alcoholate complexes.[13] In this case, the oxophilicity of the Mn^{III} ions could be held responsible for a specific binding mode of the peroxide which might be different in the $Mn^{II}Mn^{II}$ state of the enzymes. The present results show that the same chemistry is performed by a $Mn^{II}Mn^{III}$ site. Since the Mn^{II} is not oxophilic, this may be a general feature of Mn_2O_2 cores and therefore possibly valid also for the enzymatic reaction.

Although these active species are present whatever the catalyst, their ratio depends on the catalyst and changes during the catalysis. In the case of **1a**, the oxidized form **2a** dominates most of the reaction while the reduced form is clearly detected in late stages only. This is consistent with the oxidation of H_2O_2 being slower than its reduction. It is worth noting that the reverse is observed in the catalase from *L. plantarum* where the steady state comprises ca. two-thirds of the reduced form of the enzyme.[7] The more efficient reduction of H_2O_2 by the enzyme may reflect its better ability to manage the protons required in the reaction.

Acknowledgment. This research was supported in part by the COST D21 program.

Supporting Information Available: The mass spectrum of **4a** in the positive and negative ESI modes (Figures S1a,b), the mass spectrum of the catalase-like reaction of **1a** in the presence of CD_3OD (Figure S2) and of **1b** (Figure S3), and the cyclic voltammogram of **2a** (Figure S4). This material is available free of charge via the Internet at http://pubs.acs.org.

IC020646N

(63) Bhula, R.; Gainsford, G. J.; Weatherburn, D. C. *J. Am. Chem. Soc.* **1988**, *110*, 7550−7552.
(64) Bossek, U.; Weyhermüller, T.; Wieghardt, K.; Nuber, B.; Weiss, J. *J. Am. Chem. Soc.* **1990**, *112*, 6387−6388.
(65) VanAtta, R. B.; Striuse, C. E.; Hanson, L. K.; Valentine, J. S. *J. Am. Chem. Soc.* **1987**, *109*, 1425−1434.
(66) Kitajima, N.; Komatsuzaki, H.; Hikichi, S.; Osawa, M.; Moro-oka, Y. *J. Am. Chem. Soc.* **1994**, *116*, 11596−11597.